The role of cyadox and recombinant growth hormone (rGH) on the promotion of growth through epigenetics

Aimei Liu
Huazhong Agriculture University
Feng Zhu
Huazhong Agriculture University
Xiaohui Zhu
Huazhong Agriculture University
Yulian Wang
Huazhong Agriculture University
Awais Ihsan
COMSATS University Islamabad
Zhenli Liu
Huazhong Agriculture University
Menghong Dai
Huazhong Agriculture University
Xu Wang (wangxu@mail.hzau.edu.cn)
Huazhong Agriculture University

Research

Keywords: Cyadox, RGH, DNA methylation, Histone modification, Chromatin remodeling

Posted Date: May 11th, 2020

DOI: https://doi.org/10.21203/rs.3.rs-26866/v1

Abstract

Background: Cyadox is an effective growth-promoting antibiotic, which is similar to the role of recombinant growth hormone (rGH). Current studies have shown that cyadox can promote animal growth through altering intestinal microflora, improving protein utilization and increasing protein synthesis. Increasing evidence suggests that epigenetics are also closely related to growth. However, the potential role of epigenetics in the cyadox for growth has not been explored.

Results: Here, we used recombinant growth hormone (rGH) and cyadox to study the relationship between growth and changes in epigenetics including DNA methylation, histone modification and chromatin structure. Bisulfite DNA sequencing (BSP) assay suggested that cyadox and rGH treatments increased IGF-1 expression partially by hypomethylation at CpG sites within the promoter region of IGF-1, which was regulated by DNA methyltransferases (DNMTs). We also observed an enrichment of H3K4me3 and H3K27ac at the promoter regions of IGF-1 by ChIP-qPCR assay, which contributed to an increase in IGF-1 transcription. In addition, immunofluorometric assay displayed cellular accessible chromatin structure following the treatment of cyadox and rGH, facilitating the combination of transcription factors and DNA and thus enhancing gene transcription.

Conclusions: Taken together, our findings indicated that cyadox and rGH promote cell growth partially through epigenetic changes, providing a prospect for the development of animal growth-promoting drugs in the future.

Introduction

Quinoxaline, 1,4-dioxide derivatives (QdNOs), consisting of one or two acyclic chain moieties combined with a quinoxaline ring, are antibacterial and growth promoting agents and have a wide range of biological properties, including antibacterial, antitubercular, anticancer, anti-candida, and antiprotozoal [1–7]. Previous reports suggest that these drugs can alter intestinal microflora, improve protein utilization, and increase protein synthesis in vivo [1]. Cyadox (2-formylquinoxaline-N1, N4-dioxide cyanoacetyl hydrazone) belongs to QdNOs, could significantly improve growth of animals such as pigs, cattle and poultry [8–11]. Additionally, cyadox has shown antibacterial activity, with a lower toxicity in animals [12]. However, the mechanism by which cyadox induces growth remains unclear.

Increasing attention has been paid to the vital role of epigenetics in animal growth and development [13–16]. Epigenetics mainly include DNA methylation, histone modification and chromatin remodeling [17]. DNA methylation which is dynamically regulated by DNA methyltransferases (DNMTs) [18], plays a key role in maintaining normal cell differentiation and regulating gene expression [19]. For example, DNA methylation is closely associated with programmed inhibition of tissue differentiation and activation of genes involved in tissue-specific processes [19]. DNA methylation can influence the growth and development of the embryo [20], fetus and infant [21].

Additionally, different types of histone modification also have a significant impact on growth and development [22, 23]. Tri-Methyl-Histone H3 (Lys4) (H3K4me3) and Acetyl-Histone H3 (Lys27) (H3K27ac) are generally linked to gene activation and growth and development of the body [24]. H3K27ac and H3K4me3 modifications mainly occur around transcriptional start sites (TSSs) [25, 26]. At present, the research of histone modification mainly focuses on the growth, maturation and activation of germ cells such as oocytes [23] and sperm [27], and the occurrence and development of diseases [28].

DNA methylation and histone modification in the nucleus can also affect the three-dimensional structure of chromatin, thus influencing on gene expression related to growth and development [29, 30]. Chromatin remodeling can lead to changes in the position and structure of nucleosomes, leading to changes in chromatin [31]. Although, there are many studies on growth and epigenetics, but the role of DNA methylation, histone modification and chromatin remodeling in antimicrobial growth promotion remains unknown.

It is well known that growth hormone (GH) can enhance somatic growth and tissue repair [32]. Similar to the function of GH, insulin-like growth factor 1 (IGF-1) is also essential for the body's growth [33]. In present study, we used the rat liver cell line BRL because IGF-1 is mainly secreted by the liver which is the main organ of drug metabolism. DNA methylation and histone modification can control the expression of IGF-1 [34, 35]. However, the relationship between DNA methylation, histone modification of IGF-1gene and cyadox-inducing cell growth remains unclear. Thus, in present study, we used most sophisticated molecular biology techniques including quantitative real-time polymerase chain reaction (RT-PCR), western blot, bisulfite DNA sequencing (BSP), and immunofluorescence assay to illustrate the potential mechanisms.

Materials And Methods

Reagents and chemicals

Cyadox was synthesized by the Institute of Veterinary Pharmaceuticals (HZAU) (Wuhan, China). rGH was purchased from Nanjing Pharmaceutical Hubei Co. Ltd. (Wuhan, China). High-glucose DMEM was obtained from Hyclone (Logan, UT, 3 USA); fetal bovine serum (FBS), antibiotics (penicillin, streptomycin) and trypsin-EDTA 4 solutions were supplied by Gibco BRL-Life Technologies (Logan, UT, USA). 3-(4,5-dimethylthiazolyl-2)-2,5-diphenyltetrazolium bromide (MTT), bovine serum albumin (BSA), RIPA Lysis Buffer, thiourea, phenylmethanesulfonyl fluoride (PMSF), sodium dodecyl sulfate (SDS), 5-Aza-2'-deoxycytidine (DAC), Cell Genomic DNA Kit, glutamine, acrylamide, bis-acrylamide, ammonium persulfate (APS), Tris Base, DL-Dithiothreitol (DTT) and methanol were bought from Sigma (St. Louis, MO, USA). Alexa Fluor 594-conjugated Goat anti-Rabbit lgG (H + L) was purchased from Proteintech (Wuhan, China). Acetyl-Histone-H3 (Lys) (D5E4) XP Rabbit monoclonal antibody (mAb), Tri-Methyl-Histone H3 (Lys4) (C42D8) Rabbit mAb and β-Actin Rabbit mAb were purchased from Cell Signaling Technology (Mass, USA). DL2000 DNA™ Marker, dNTP Mixture (10 mM), M-MLV RTase, 5 × M-MLV Buffer, Oligo d(T)18, DNA Ligation Kit Ver.2.1, T-Vector pMD19 (simple), RNAiso Plus, RNA Nase, SYBR Premix Ex Taq™ (Perfect

Real Time), TaKaRa Taq™ were bought from TaKaRa Biotechnology Co., Ltd. (Dalian, Liaoning, P.R. China). DAPI Staining Solution, Antifade Mounting Medium and Blocking Buffer were bought from Beyotime (Wuhan, P.R. China). The Simple ChIP Enzymatic Chromatin IP Kit (Magnetic Beads) was purchased from Cell Signaling Technology (Mass, USA). MethylFlash Methylated DNA Quantification Kit (Colorimetric) was purchased from Epigentek (Farmingdale, NY, USA). The EZ DNA Methylation-Gold™ Kit was purchased from Zymo Research Corp (Orange, CA, US).

BRL cell culture and treatment

BRL cells were procured from the Cell Bank of Type Culture Collection at the Chinese Academy of Sciences. BRL cells were cultured in high-glucose Dulbecco's modified Eagle's medium (DMEM) medium supplemented with 10% fetal serum (FBS, Gibco), 2 mM glutamine, 100 U/mL penicillin and 100 μg/mL streptomycin at 37℃ with an atmosphere of 5% CO_2. BRL cells passaged 5 ~ 15 times were used in the experiments. All experiments were performed at least in triplicate on three separate occasions.

Cell viability assay

Cells treated with cyadox at different concentrations (0, 1, 2, 4, 6, 8, and 10 μM) were seeded onto 96-well plates with 1×10^5/mL cells per well and then incubated at 37℃ for 0.5, 1, 2, 4, 8, 12, and 24 h, respectively. After incubation, the cells were treated with 0.5 mg/mL solution of MTT (20 μL/well) at 37℃ for 4 h. Next, after discarding the supernatants of each well, 150 μL of dimethylsulfoxide (DMSO) was added to dissolve the purple formazan crystals. After 10 min, the optical density (OD) was read on a microplate reader (Bio-Tek Instruments, Inc., Winooski, VT, USA). The results were calculated as: the relative viability of cell = (OD of the sample well – OD of the blank well) / (OD of control well – OD of the blank well) × 100%. Sample well: pore with cell, MTT solution and drug solution; blank well: a cell-free pore with a medium and MTT solution; control well: pore with cell, MTT solution but without drug solution. From these data, we established the optimal culture time and cyadox concentration. Then, We tested nine concentrations of rGH (1.59×10^{-4}, 3.18×10^{-4}, 6.37×10^{-4}, 1.27×10^{-3}, 2.55×10^{-3}, 5.09×10^{-3}, 1.02×10^{-2}, 2.04×10^{-2} and 4.08×10^{-2} IU/mL) using the same method and conditions as above.

RNA extraction and RT-PCR assay

BRL cells grown to near confluence in 12-well plates were subjected to serum-free medium for 12 h of starvation. The serum-free DMEM medium was replaced with serum-free DMEM medium containing cyadox (1 μM) and rGH (6.37×10^{-4} IU/mL). After 0.5, 1, 2 and 4 h, total RNA was extracted from cells using RNAiso plus (TaKaRa, Japan) according to the manufacturer's instructions. Reverse transcription was performed on 1 μg of total RNA by using a PrimeScript RT reagent kit. CDNAs obtained were diluted and used for RT-PCR.

The transcript levels of growth hormone receptor (GHR), IGF-1 and insulin-like growth factor 1 receptor (IGF-1R) genes were detected by RT-PCR. To investigate the relationship between growth and epigenetics, we also measured the transcript levels of DNA methyltransferase 1 (DNMT1), DNA methyltransferase 3A (DNMT 3A) and DNA methyltransferase 3B (DNMT 3B) (DNA methylation related genes); lysine

demethylase 5A (Kdm 5a), lysine demethylase 5B (Kdm 5b) and lysine methyltransferase 2A (Kmt 2a) (H3K4me3 related genes); and CREB binding protein (Crebbp), lysine acetyltransferase 2A (Kat 2a), lysine acetyltransferase 2B (Kat 2b), and histone deacetylase 1 (HDAC1) (H3K27ac related genes). Primers were designed with Primer Premier 5.0 software corresponding to the cDNA sequences (Table 1). Each 20 μL reaction mixture consisted of 10 μL SYBR® Premix Ex Taq™, 0.4 μL of each primer (10 μM), 2.0 μL of cDNA, and 7.2 μL Rnase Free H_2O. For all primers, the cycling conditions were as follows: step 1, 30 s at 95℃; step 2, 45 cycles at 95℃ for 5 s, 55 ~ 60℃ for 30 s; step 3, dissociation stage. In this study, the housekeeping gene β-actin was used as the internal calibrator reference gene for expression profiling of genes. Data were analyzed and quantified using the $2^{-\Delta\Delta Ct}$ method [36].

Table 1
The sequences of primers used for RT-PCR analysis

Gene	Accession number	DNA sequence (5'to 3')	Product size (bp)
β-actin	NM_031144.3	Forward: GAGATTACTGCCCTGGCTCCTA	148
		Reverse: ACTCATCGTACTCCTGCTTGCTG	
IGF-1	NM_001082477.2	Forward: TACTTCAACAAGCCCACAGG	123
		Reverse: CAGCGGAGCACAGTACATCT	
IGF-1R	NM_052807.2	Forward: ATCAGGCTTCATCCGCAACA	246
		Reverse: TTCACGTAGCCAGTCACCAC	
GHR	NM_017094.1	Forward: GTCCGAGACAGCAGATACCG	98
		Reverse: TCGCGTTGAGTATAAGGCCC	
DNMT 1	NM_053354.3	Forward: GCTGTTCCTTGTAGGCGAGT	201
		Reverse: GGGGACTCAAACCTTGCGTA	
DNMT 3A	NM_001003958.1	Forward: CCCAGAAAGAGCACAACAGA	113
		Reverse: CAAATGTCCTCGATGTTTCG	
DNMT 3B	NM_001003959.1	Forward: ACAACCATTGACTTTGCCGC	107
		Reverse: CGTTCTCGGCTCTCCTCATC	
Kat 2a	NM_001107050.1	Forward: GAGGCCCCTGACTACTACGA	101
		Reverse: ACAAAGAGCTTCCGGGTCAC	
Kat 2b	XM_003750617.4	Forward: GAGTGAACGCCTCAGGAACA	122
		Reverse: TGGCGCACTTGTAGTACTCG	
Crebbp	NM_133381.3	Forward: AGGCAGGTGTTTCACAGCTT	94
		Reverse: TGGGAACTGGTTTCAGCACT	
HDAC 1	NM_001025409.1	Forward: TGACCAAGTACCACAGCGAC	264
		Reverse: AACAGAAGCCGGATGCTTCA	
Kmt 2a	XM_008766179.1	Forward: TCTGGATGGGTCGTCATCCT	225
		Reverse: GGTTCGGCAAAAGTGCCAAT	
Kdm 5a	NM_001277177.1	Forward: GTCACCCGAAGACGGAAAGT	158
		Reverse: CACCCGTCACACAAAAGCAG	
Kdm 5b	NM_001107177.1	Forward: CGCGTGCCAGTGTTAGAAAC	191

Gene	Accession number	DNA sequence (5'to 3')	Product size (bp)
		Reverse: TCACACCGAGGACAAAGAACC	

Genome 5-methylcytosine (5-mC) level and promoter region methylation level of IGF-1

To illustrate whether genomic 5-mC level is affected by cyadox and rGH, BRL cell DNA was extracted using a DNA isolation kit following treatment with either cyadox or rGH. A MethylFlash Methylated DNA Quantification Kit (Colorimetric) was then used to detect DNA methylation level. DNA methylation level in the promoter CpG sites of IGF-1 gene was checked by BSP. Primers (Table 2) were designed by MethPrimer 2.0.

Table 2
The sequences of primers used for BSP (Bisulfite sequencing)

Gene	DNA sequence (5'to 3')	Product size (bp)
IGF-1 B1	Forward: AAATTGGATTAATAAAAGATTAGAA	103
	Reverse: AATAACTAACAACATAACTCAAACC	
IGF-1 B3	Forward: AAGGTTTTGGTGGATTATTTTTTTT	174
	Reverse: ATCCCTACTCATACAATAACCCAAA	
IGF-1 B5	Forward: TTTTTTTGTTTGTTAAATTTTATTGT	208
	Reverse: TAAAAAACTACTAATTTTCCCCATC	

Note: BSP: bisulfite sequencing PCR. IGF-1 B1, IGF-1 B3 and IGF-1 B5 were three regions most likely to undergo DNA methylation changes in the IGF-1 promoter region predicted by MethPrimer 2.0. And a total of 5 regions were predicted, but IGF-1 B1, IGF- 1 B2 and IGF-1 B4 had the same CpG sites in the IGF-1 promoter region, IGF-1 B1 was selected for the corresponding experiment.

Western blot assay

BRL cells (1×10^5/mL) were seeded in 6-well plates and incubated respectively with 1 μM cyadox and 6.37×10^{-4} IU/mL rGH for 0.5, 1, 2 and 4 h. Total protein was isolated in a preparation of radio immunoprecipitation assay (RIPA) lysis buffer, then a sonic oscillator was used to break the cells or organelles. The concentration of proteins was quantified by bicinchoninic acid (BCA) assay (Beyotime, PR, China). Equal amounts of protein were separated by SDS-PAGE electrophoresis (12.5%) and transferred to nitrocellulose membranes (Millipore, Bedford, MA, USA). The blots were blocked and then labeled with primary antibodies to Acetyl-Histone-H3 (Lys) (D5E4) XP Rabbit monoclonal antibody (mAb) (CST, USA), Tri-Methyl-Histone H3 (Lys4) (C42D8) Rabbit mAb (CST, USA) and β-actin overnight at 4°C. After washing, blots were incubated for 1 h with the corresponding secondary antibody at a 1:5000 dilution. Immunoreactive bands were detected using the Luminata Classico Western HRP Substrate Kit

(Millipore, Bedford, MA, USA), and signal intensity and images were captured with an LAS-4000 luminescent image analyser (Fujifilm, Tokyo, Japan).

ChIP-qPCR assay

ChIP-qPCR was used to found the amount of H3K4me3 and H3K27ac in the promoter of IGF-1 gene in BRL cells treated with either 1 μM cyadox or 6.37×10^{-4} IU/mL rGH for 4 h. The ChIP assay was completed using the SimpleChIP® Enzymatic Chromatin IP Kit (Magnetic Beads) (CST, USA). The qPCR primers used for the ChIP analysis were shown in Table 3.

Table 3
The sequences of primers used for ChIP-qPCR analysis

Gene	DNA sequence (5'to 3')	Product size (bp)
-1036	Forward: AGCAGGTCTGGCTCATTTCCAT	78
	Reverse: AGATCAGATGCTGCGCTTTCCA	
-541	Forward: TAGTGTGTGCCTCCCATACTGCTT	105
	Reverse: TGAGCTCTGGGACAGTCTGAAA	
+ 10	Forward: AAACGCCTCTGTGCTCCAGTTT	104
	Reverse: TCTCTCTCCCTCTTCTGGCAAAGT	
+ 1291	Forward: TCTCCTTTCGATCACTGGACCT	105
	Reverse: TGACAGCGGCTTAGAAGTGCTTG	
+ 2232	Forward: ACCCACTCTGACCTGCTGTGTAAA	86
	Reverse: AGGGCAACAGTTGTAAGAGGGT	
+ 2850	Forward: TGGACTTAAATGCACCGTCCCT	98
	Reverse: TGTTACTCAGCCTCACAGCCTT	

Immunofluorescence assay

To investigate chromatin loosening changes after treatment of rGH (6.37×10^{-4} IU/mL, 4 h), cyadox (1 μM, 4 h), rGH (6.37×10^{-4} IU/mL) and inhibitor (DAC, 5 μM, Sigma, USA) for 4 h, cyadox (1 μM) and inhibitor for 4 h and 1,4-Bidesoxycyadox (1 μM) (HZAU, Wuhan, China) for 4 h, BRL cells were placed onto 25 mm coverslips in 6-well plates. The cells without drugs treatment were used as negative control. After drugs treatment, cells were fixed in 4% paraformaldehyde for 15 min at 37℃ and permeabilized for 3 min at -20℃ with Triton X-100 (0.5% v/v). After washing with PBS twice, cells were saturated with 5% BSA (Sigma, USA) for 30 min and incubated with primary antibody (H3K4me3 and H3K27ac) overnight at 4℃. Secondary antibody, the mixture including donkey anti-goat IgG conjugated with Alexa Fluor® 488 and donkey anti-rabbit IgG with Alexa Fluor® 594 (Cell Signaling Technology), was added for 1 h at 37℃

in the dark. All of the above-cited antibodies were diluted in 1% PBS. Then, the cells were incubated in DAPI (5 μM, Invitrogen) staining solution for 5 min and washed in PBS to monitor cellular fluorescence with an UltraVIEW VOX Confocal system (PerkinElmer, Co., Norwalk, Conn., USA) using a 60×, 1.4 NA oil immersion objective lens.

Statistical analysis

Data were analyzed by SPSS 16.0 for Windows. All results were presented as means ± standard deviation (SD). Compared with control group, significant differences were indicated by $*p < 0.05$.

Results

Analysis of MTT

As shown in Fig. 1A, the cell viability of cyadox (1 μM) treatment was the highest in 4 h. When cyadox (1 μM) treated cells for more than 4 hours, the cell viability decreased, which may be due to the increased toxicity of drugs to cells as the time of drug treatment increased; on the other hand, high concentration cyadox (higher than 1 μM) is toxic to cells. Therefore, it was observed the viability was the highest after cyadox (1 μM) treatment for 4 h. And one study revealed that cyadox (1 μM for 4 h) could enhance growth of porcine primary hepatocytes [6]. Thus, the subsequent experiments were performed using 1 μM cyadox for 4 h.

BRL cells viability was measured by MTT assay after treatment with a range of rGH concentrations between 1.59×10^{-4} and 4.08×10^{-2} IU/mL for 4 h (Fig. 1B). Cell viability was higher when cells were exposed to 6.37×10^{-4} IU/mL rGH for 4 h than for the other tested concentrations. Based on these results, we concluded that incubation with 6.37×10^{-4} IU/mL rGH for 4 h was more conducive to cell growth.

Cyadox and rGH enhance the expression of IGF-1 gene

As shown in Fig. 1, IGF-1 transcript levels were higher after treatment with either cyadox (1 μM) or rGH (6.37×10^{-4} IU/mL) for 4 h, compared to the control group. GH and IGF-1 receptors such as GHR and IGF-1R were also increased to varying degree after treatment with cyadox (1 μM) or rGH (6.37×10^{-4} IU/mL) for 0.5, 1, 2, 4 h (Fig. 1C ~ 1G). IGF-1 is likely to be an important target of rGH and cyadox and related to cell growth.

Promoter hypomethylation mediates upregulation of IGF-1 under rGH and cyadox

Furthermore, we also tested whether rGH and cyadox affected genomic DNA methylation level in BRL cells. We found that cyadox and rGH increased 5-mC levels compared to control group. This effect could be reversed by the addition of DNA methylation inhibitors, DAC (Fig. 2A). The expression of DNMTs regulated the level of 5-mC level was a dynamic change. As shown in Fig. 2F ~ 2K, gene expression of DNMT1 significantly increased than control group after BRL cells were exposed to 1 μM cyadox or 6.37 ×

10^{-4} IU/mL rGH for 4 h, respectively, which agreed well with 5-mC levels. DNMT 3A and DNMT 3B expression also increased to varying degrees after cells were treated with cyadox and rGH for different times.

To further investigate DNA methylation level in the promoter regions of IGF-1 influenced by rGH and cyadox, the BSP was used to detect 10 CpG sites (Fig. 2B–E). Among them, methylation levels of CpG sites (-1314, -1284, -1229, -1227, -2) of IGF-1 promoter regions significantly decreased under rGH and cyadox. Additionally, the methylation level of CpG site (-128) was lower than control group after rGH treatment in BRL cells. These results indicated that rGH and cyadox reduced the expression of IGF-1 by partially DNA hypomethylation.

Histone modification participates in high expression of IGF-1 under rGH and cyadox

To investigate the relationship between expression of IGF-1 and histone modification, H3K27ac and H3K4me3 levels were detected by western blot after cells were exposed to cyadox and rGH, respectively (Fig. 3A). The total gray value related to H3K27ac (Fig. 3B) and H3K4me3 (Fig. 3C) was analyzed by software of Image J. We found that the level of β-actin was similar in all treatments. The levels of H3K27ac and H3K4me3 were also similar at different times in control group. The levels of H3K27ac and H3K4me3 decreased following cyadox treatment (1 μM) or rGH treatment (6.37×10^{-4} IU/mL) for 4 h. By ChIP-qPCR, we found that positions around the promoter 1 and promoter 2 regions of IGF-1 were enriched with H3K27ac and H3K4me3 following cyadox and rGH treatments (Fig. 3D). The same trend was observed for H3K4me3 (Fig. 3E). H3K27ac and H3K4me3 are related to gene activation. Our results suggested that the level of H3K27ac was increased significantly at the sites − 1036, -541, + 10, +1291, + 2232 and + 2850 when BRL cells were treated with cyadox or rGH. The level of H3K4me3 was increased significantly at the sites − 1036, -541, + 1291, +2232 and + 2850 when BRL cells were treated with cyadox, and at the sites − 1036, -541, + 10, +1291, and + 2232 when BRL cells were treated with rGH. The high level of H3K27ac and H3K4me3 on promoter 1 and promoter 2 of IGF-1 can relax the chromatin and increase transcription levels. In addition, H3K4me3 and H3K27ac can be regulated by Kdm 5a, Kdm 5b, Kmt 2a, and Crebbp, Kat 2a, Kat 2b, HDAC1, respectively. As shown in Fig. 4, these genes mRNA levels presented a dynamic expression in the period of 0.5 ~ 4 h after BRL cells were exposed to 1 μM cyadox or 6.37×10^{-4} IU/mL rGH, indicating drugs may regulate histone modification level of IGF-1 gene by disrupting gene expression related to histone modification.

Cyadox and rGH alter the chromatin status of BRL cells

Histone modification is mainly enriched on chromatin. To confirm the effect of cyadox and rGH on the state of chromatin loosening in BRL cells, we carried out immunofluorescence analysis using H3K27ac and H3K4me3 antibodies. The results about H3K27ac suggested that the gaps among nucleosomes were wider and chromatin was lost when cells were exposed to cyadox or rGH. However, when DAC was added to the culture medium together with rGH or cyadox, it showed contrary results (Fig. 5C4, 5C5). In addition,

the main metabolite of cyadox, 1, 4-Bidesoxycyadox could also not change gaps among nucleosomes (Fig. 5C6) and couldn't make chromatin loose.

Results of H3K4me3 immunofluorescence displayed that the gaps among nucleosomes were wider, and chromatin was looser when cells were exposed to rGH. Cyadox did not make the chromatin loose compared with the control group. Moreover, when DAC was added to the culture medium together with rGH or cyadox, the visible gaps formed in the nucleus were larger, and the space between the whole chromosomes in the nucleus was smaller (Fig. 6C4, 6C5). In addition, 1, 4-Bidesoxycyadox and couldn't make chromatin loose (Fig. 6C6). Based on the above results, we speculated chromatin remodeling was involved in the growth-promoting mechanisms of both drugs.

Discussion

Our results demonstrated that rGH and cyadox affected DNA methylation and histone modification of IGF-1 gene promoter. In addition, these two drugs can also affect the state of chromatin loosening in BRL cells. These findings shed new light on the relationships between epigenetics and body's growth.

Currently, quite many studies have suggested that cyadox can improve the growth performance of animals including pigs and poultry [6, 7, 37–40]. Antimicrobials including cyadox might influence growth via an endocrine axis such as IGF-1, GH and epidermal growth factor (EGF) [41]. One study has found that pigs given 50 mg/kg cyadox diet showed the greater average daily gain (ADG) and the better food efficiency compared with given 0 mg/kg cyadox diet [41]. Interestingly, pigs given 50 mg/kg cyadox diet had higher EGF concentrations than pigs given control diet throughout the experiment [41]. EGF is known to exert different biological actions *in vivo* and *in vitro* influencing the proliferation [42, 43], differentiation [44, 45]. Additionally, the insulin concentrations increased after the beginning of cyadox treatment and reached a peak at the level of 50 mg/kg in the weeks [41]. Insulin also stimulates hepatic IGF-1 release [46, 47]. As known, the increase of IGF-1 expression can promote cell proliferation and differentiation in cells [48, 49]. In present study, cyadox also increased cell viability and enhanced the expression of IGF-1 in BRL cells, which suggests that cyadox may promote cell proliferation partially through high expression of IGF-1 gene.

DNA methylation is an important growth-promoting mechanism of cyadox and rGH. Although, there are many studies suggested that cyadox as growth promoting agent, however, those were focused on the changes of intestinal microorganisms and apparent digestibility of nutrients [50]. In recent years, the role of DNA methylation in animal growth has gained extensive attention. DNA methylation mainly takes place in CpG dinucleotides, adding a methyl group to the cytosine to form 5-mC [51]. DNA methylation is closely related to increased gene expression, whereas hypermethylation usually leads to inhibition of genes expression [52]. DNA methylation can regulate several biological events, including X-chromosome inactivation, embryonic development, genomic imprinting, transcriptional regulation, and chromatin modification [53]. However, the role of DNA methylation in cyadox-induced growth is unknown. The present study demonstrated that cyadox and rGH induced genome-wide DNA hypermethylation, which is

regulated by DNMT1. Hypermethylation is usually not harmful, whereas hypomethylation typically leads to growth arrest or apoptosis in mammalian cells [54]. Thus, the proper hypermethylation in cells is thought to be beneficial for growth and development. To our knowledge, this is the first study to demonstrate the effects of rGH and Cyadox on whole genome 5-mC level. Importantly, we found that DNA methylation level of IGF-1 promoter was reduced in different extent at ten CpG sites after rGH and cyadox treatments, which facilitates the transcription of IGF-1, increasing IGF-1 expression. These findings indicated that IGF-1 expression would be increased due to local hypomethylation under rGH and cyadox, which is in line with the findings of a report [55].

DNA methylation is regulated by DNMTs mainly DNMT1, DNMT 3A, DNMT 3B. DNMTs use S-adenosylmethionine (SAM) as a methyl donor to catalyze a methyl group to add to the cytosine ring to form methylcytosine [56]. DNMT1 is responsible for the restoration of hemimethylated to full methylation (maintenance methylation) and is the predominant mammalian DNA methylating enzyme. DNMT 3A and DNMT 3B create new DNA methylation sites (*de novo* methylation) [57]. In present study, the gene expression of DNMTs (DNMT1, DNMT 3A) decreased first and then increased in the time effect of cyadox and rGH. This may be responsible for maintaining cell homeostasis through demethylation during the compensatory process; and then with the continuous stimulation of drugs, drugs may downregulate certain genes through hypermethylation, and thus play its own pharmacological role. Although the mRNA lever of DNMT1 and DNMT 3A genes significantly increased than control group after BRL cells were exposed to 1 μM cyadox for 4 h, it only reflects genome-wide methylation level in cells. After the drug acts on the cells, some genes may be hypermethylated and others may be hypomethylated or unchanged.

H3K4me3 and H3K27ac can induce gene activation and play an important role in the growth [24]. However, little known about how rGH and cyadox affect H3K27ac and H3K4me3 levels. Present study found that the H3K27ac and H3K4me3 levels are reduced by cyadox and rGH treatments. Modified histones can interact with other proteins to affect gene expression [58]. Histone acetylation can activate gene transcription and mainly occurs in lysines [59]. Histone methylation can regulate the chromatin structure and growth of the cells, and mainly occurs in lysine and arginine residues [60]. The decreased level of total H3K27ac and H3K4me3 in BRL cells exposed to cyadox and rGH may be the result of the combination of different genomic protein modifications. Cyadox and rGH can increase the levels of H3K4me3 and H3K27ac around promoter 1 and promoter 2 of IGF-1, inducing IGF-1 expression. Some active enhancers are usually marked by H3K27ac, which is around transcriptional start sites (TSSs) [25, 26, 61, 62]. Some active enhancers are also associated with H3K4me3, which is related to RNA polymerase II activity [63]. Thus, modification of H3K4me3 might enable the activity of RNA polymerase II, thus increasing IGF-1 transcription initiation. In addition, the increased level of H3K27ac was first to be found in promoter 1 and promoter 2 of IGF-1 when the BRL cells were treated with rGH and cyadox, respectively.

Histone methylation can be regulated Kdm 5a, Kdm 5b [64] and Kmt 2a [65]. Kdm 5a and Kdm 5b can inhibit H3K4me3 [66], however, Kmt 2a, a methyltransferase, can activate H3K4me3 [67]. We found that cyadox and rGH increased the level of Kdm 5a and Kdm 5b expression. The high expression of Kdm 5a

and Kdm 5b and low expression of Kmt 2a caused the low level of H3K4me3 in BRL cells under cyadox and rGH. Additionally, Histone acetylation can be regulated by genes of Crebbp [68], Kat 2a [69], Kat 2b [70] and HDAC1 [71]. Crebbp, Kat 2a, and Kat 2b are histone acetyltransferase, and HDAC1 is a histone deacetylase. Our present results suggested that cyadox and rGH downregulated the level of Kat 2a and Crebbp, and increased HDAC1 expression, which could lower the H3K27ac level in cells.

Chromatin structure is closely related to gene activation and inhibition in cells [72]. The current results displayed that the visible space in the nucleus was smaller and gaps among nucleosomes were wider after BRL cells were treated with rGH and cyadox, which may be caused by DNA methylation and histone modification changes [73]. These results indicated that rGH and cyadox loosens the chromatin of BRL cells, facilitating transcriptional activation of growth-related genes.

Conclusion

In summary, our research (Fig. 7) revealed that cyadox and rGH elevated IGF-1 expression via hypomethylation and the enrichment of H3K4me3, H3K27ac in the promoter region of IGF-1. Additionally, accessible chromatin structure of BRL cells induced by cyadox and rGH is conducive to genes transcription and promotes cell growth. Taken together, the current data provide a novel insight for drugs-induced growth of animals from the perspective of epigenetic changes, contributing to future research in the field.

Abbrevations

5-mC, 5-methylcytosine; AP, ammonium persulfate; BCA, bicinchoninic acid; BRL cells, rat normal liver cells; BSP, Bisulfite DNA sequencing; BSA, bovine serum albumin; C, cytosine; CpG, cytosine-phosphate-guanine; ChIP, Chromatin immunoprecipitation; Crebbp, CREB binding protein; DTT, DL-Dithiothreitol; DMEM, dulbecco's modified eagle medium; DMSO, dimethylsulfoxide; DNMTs; DNA methyltransferases; DNMT1, DNA methyltransferase 1; DNMT 3A, DNA methyltransferase 3A; DNMT 3B, DNA methyltransferase 3B; ECL, enhanced chemiluminescence; EGF, epidermal growth factor; FBS, fetal bovine serum; G, guanine; GH, growth hormone; GHR, growth hormone receptor; H3K27ac, Acetyl-Histone H3 (Lys27); H3K4me3, Tri-Methyl–Histone H3 (Lys4); HDAC1, histone deacetylase 1; IGF-1, insulin-like growth factor 1; IGF-1R, insulin-like growth factor 1 receptor; IUGR, intrauterine growth retardation; Kdm 5a, lysine demethylase 5A; Kdm 5b, lysine demethylase 5B; Kmt 2a, lysine methyltransferase 2A; Kat2a, lysine acetyltransferase 2A; Kat2b, lysine acetyltransferase 2B; MTT, 3-(4, 5-dimethylthiazolyl-2)-2,5-diphenyltetrazolium bromide; OD, optical density; PMSF, phenylmethanesulfonyl fluoride; PVDF, polyvinylidene fluoride; QdNOs, quinoxaline 1,4-di-N-oxide derivatives; rGH, recombinant growth hormone; SDS, sodium dodecyl sulfate; SAM, S-adenosylmethionine; SAH, S-adenosyl-L-homocysteine; TSSs, transcriptional start sites; UQ, ubiquinone.

Declarations

Acknowledgements

Not applicable.

Authors' contributions

Conception and design: Aimei Liu; Financial support and designed research: Aimei Liu, Feng Zhu, Xu Wang and Menghong Dai; Performed research and analysed data: Aimei Liu, Feng Zhu, Xiaohui Zhu, Yulian Wang, Awais Ihsan, Zhenli Liu, Menghong Dai, and Xu Wang. All authors have read and approved the final manuscript.

Funding

This work was supported by National Key R & D Program of China (2018YFC1603005), Applied Basic Research Programs of Wuhan (grant no. 2017020201010228), and the Fundamental Research Funds for the Central Universities (grant no. 2662017JC034).

Availability of data and materials

The data sets used and analyzed during the current study are available from the corresponding author on reasonable request.

Ethics approval and consent to participate

Not applicable.

Consent for publication

Not applicable.

Competing interest

The authors declare that they have no competing interests.

References

1. Carta A, Corona P, Loriga M. Quinoxaline 1,4-dioxide: a versatile scaffold endowed with manifold activities. Curr Med Chem. 2005;12(19):2259-2272.
2. Vicente E, Perez-Silanes S, Lima LM, Ancizu S, Burguete A, Solano B, et al. Selective activity against Mycobacteriumtuberculosis of new quinoxaline 1,4-di-N-oxides. Bioorg Med Chem. 2009;17(1):385-389.
3. Ihsan A, Wang X, Liu Z, Wang Y, Huang X, Liu Y, et al. Long-term mequindox treatment induced endocrine and reproductive toxicity via oxidative stress in male Wistar rats. Toxicol Appl Pharmacol. 2011;252(3):281-288.

4. Wang X, He QH, Wang YL, Ihsan A, Huang LL, Zhou W, et al. A chronic toxicity study of cyadox in Wistar rats. Regul Toxicol Pharmacol. 2011;59(2):324-333.
5. Wang X, Zhang H, Huang L, Pan Y, Li J, Chen D, et al. Deoxidation rates play a critical role in DNA damage mediated by important synthetic drugs, quinoxaline 1,4-dioxides. Chem Res Toxicol. 2015;28(3):470-481.
6. Guo J, Cui LQ, Lu QR, Zhang YF, Liu QY, Wang X, et al. Cyadox regulates the transcription of different genes by activation of the PI3K signaling pathway in porcine primary hepatocytes. J Cell Biochem. 2019;120(5):7623-7634.
7. Liu QY, Lei ZX, Zhou KX, Yu HR, Liu SH, Sun QL, et al. N-O Reduction and ROS-Mediated AKT/FOXO1 and AKT/P53 Pathways Are Involved in Growth Promotion and Cytotoxicity of Cyadox . Chem Res Toxicol. 2018;31(11):1219-1229.
8. Ding X, Yuan ZH, Wang YL, Zhu HL, Fan SX. Olaquindox and cyadox stimulate growth and decrease intestinal mucosal immunity of piglets orally inoculated with Escherichia coli. J Anim Physiol an N. 2006;90(5-6):238-243.
9. Cheng GY, Sa W, Cao C, Guo LL, Hao HH, Liu ZL, et al. Quinoxaline 1,4-di-N-Oxides: Biological Activities and Mechanisms of Actions. Frontiers in Pharmacology. 2016;7.
10. Broz J, Sevcik B. Estimation of Optimal Effective Dose of Growth Promotant Cyadox in Piglet Rearing. Biol Chem Zivocisme. 1979;15(4):319-325.
11. Broz J, Sevcik B. Efficiency of Growth Promotant Cyadox in Broilers. Arch Geflugelkd. 1980;44(3):95-98.
12. Sattar A, Xie S, Huang L, Iqbal Z, Qu W, Shabbir MA, et al. Pharmacokinetics and Metabolism of Cyadox and Its Main Metabolites in Beagle Dogs Following Oral, Intramuscular, and Intravenous Administration. Front Pharmacol. 2016;7:236.
13. Lundh T, Udagawa J, Hanel SE, Otani H. Cross- and triple-ratios of human body parts during development. Anat Rec (Hoboken). 2011;294(8):1360-1369.
14. Saintilan R, Brossard L, Vautier B, Sellier P, Bidanel J, van Milgen J, et al. Phenotypic and genetic relationships between growth and feed intake curves and feed efficiency and amino acid requirements in the growing pig. Animal. 2015;9(1):18-27.
15. Branum SR, Yamada-Fisher M, Burggren W. Reduced Heart Rate and Cardiac Output Differentially Affect Angiogenesis, Growth, and Development in Early Chicken Embryos (Gallus domesticus). Physiological and Biochemical Zoology. 2013;86(3):370-382.
16. Riley DG, Burke JM, Chase CC, Coleman SW. Heterosis and direct effects for Charolais-sired calf weight and growth, cow weight and weight change, and ratios of cow and calf weights and weight changes across warm season lactation in Romosinuano, Angus, and F-1 cows in Arkansas. Journal of Animal Science. 2016;94(1):1-12.
17. Egger G, Liang GN, Aparicio A, Jones PA. Epigenetics in human disease and prospects for epigenetic therapy. Nature. 2004;429(6990):457-463.

18. Fang X, Corrales J, Thornton C, Scheffler BE, Willett KL. Global and gene specific DNA methylation changes during zebrafish development. Comp Biochem Physiol B Biochem Mol Biol. 2013;166(1):99-108.
19. Slieker RC, Roost MS, van Iperen L, Suchiman HED, Tobi EW, Carlotti F, et al. DNA Methylation Landscapes of Human Fetal Development. Plos Genetics. 2015;11(10): e1005583.
20. Tomizawa S, Nowacka-Woszuk J, Kelsey G. DNA methylation establishment during oocyte growth: mechanisms and significance. Int J Dev Biol. 2012;56(10-12):867-875.
21. Bouwland-Both MI, van Mil NH, Stolk L, Eilers PHC, Verbiest MMPJ, Heijmans BT, et al. DNA Methylation of IGF2DMR and H19 Is Associated with Fetal and Infant Growth: The Generation R Study. Plos One. 2013;8(12): e81731.
22. Graves HK, Wang PP, Lagarde M, Chen ZH, Tyler JK. Mutations that prevent or mimic persistent post-translational modifications of the histone H3 globular domain cause lethality and growth defects in Drosophila. Epigenet Chromatin. 2016;9: 9.
23. Hoffmann S, Tomasik G, Polanski Z. DNA Methylation, Histone Modifications and Behaviour of AKAP95 during Mouse Oocyte Growth and Upon Nuclear Transfer of Foreign Chromatin into Fully Grown Prophase Oocytes. Folia Biol-Krakow. 2012;60(3-4):163-170.
24. Hennighausen L, Robinson GW. Interpretation of cytokine signaling through the transcription factors STAT5A and STAT5B. Genes & Development. 2008;22(6):711-721.
25. Rada-Iglesias A, Bajpai R, Swigut T, Brugmann SA, Flynn RA, Wysocka J. A unique chromatin signature uncovers early developmental enhancers in humans. Nature. 2011;470(7333):279-283.
26. Spicuglia S, Vanhille L. Chromatin signatures of active enhancers. Nucleus-Austin. 2012;3(2):126-131.
27. Perez-Cerezales S, Ramos-Ibeas P, Lopez-Cardona A, Pericuesta E, Fernandez-Gonzalez R, Pintado B, et al. Elimination of methylation marks at lysines 4 and 9 of histone 3 (H3K4 and H3K9) of spermatozoa alters offspring phenotype. Reprod Fert Develop. 2017;29(4):740-746.
28. Shafabakhsh R, Aghadavod E, Ghayour-Mobarhan M, Ferns G, Asemi Z. Role of histone modification and DNA methylation in signaling pathways involved in diabetic retinopathy. J Cell Physiol. 2019;234(6):7839-7846.
29. Langst G, Manelyte L. Chromatin Remodelers: From Function to Dysfunction. Genes (Basel). 2015;6(2):299-324.
30. Kang H, Ma J, Wu D, Shen WH, Zhu Y. Functional Coordination of the Chromatin-Remodeling Factor AtINO80 and the Histone Chaperones NRP1/2 in Inflorescence Meristem and Root Apical Meristem. Frontiers in plant science. 2019;10:115.
31. Zhou ZH, Wang QL, Mao LH, Li XQ, Liu P, Song JW, et al. Chromatin accessibility changes are associated with enhanced growth and liver metastasis capacity of acid-adapted colorectal cancer cells. Cell cycle. 2019;18(4):511-522.
32. Chia DJ, Young JJ, Mertens AR, Rotwein P. Distinct alterations in chromatin organization of the two IGF-I promoters precede growth hormone-induced activation of IGF-I gene transcription. Mol

Endocrinol. 2010;24(4):779-789.

33. Ashpole NM, Sanders JE, Hodges EL, Yan H, Sonntag WE. Growth hormone, insulin-like growth factor-1 and the aging brain. Exp Gerontol. 2015;68:76-81.
34. Tosh DN, Fu Q, Callaway CW, McKnight RA, McMillen IC, Ross MG, et al. Epigenetics of programmed obesity: alteration in IUGR rat hepatic IGF1 mRNA expression and histone structure in rapid vs. delayed postnatal catch-up growth. Am J Physiol Gastrointest Liver Physiol. 2010;299(5):G1023-1029.
35. Fu Q, McKnight RA, Yu X, Wang L, Callaway CW, Lane RH. Uteroplacental insufficiency induces site-specific changes in histone H3 covalent modifications and affects DNA-histone H3 positioning in day 0 IUGR rat liver. Physiol Genomics. 2004;20(1):108-116.
36. Liu XL, Huang DY, Guo P, Wu QH, Dai MH, Cheng GY, et al. PKA/CREB and NF-kappa B pathway regulates AKNA transcription: A novel insight into T-2 toxin-induced inflammation and GH deficiency in GH3 cells. Toxicology. 2017;392:81-95.
37. Ding MX, Yuan ZH, Wang YL, Zhu HL, Fan SX. Olaquindox and cyadox stimulate growth and decrease intestinal mucosal immunity of piglets orally inoculated with Escherichia coli. J Anim Physiol Anim Nutr (Berl). 2006;90(5-6):238-243.
38. Wang Y, Yuan Z, Zhu H, Ding M, Fan S. Effect of cyadox on growth and nutrient digestibility in weanling pigs. S Afr J Anim Sci. 2005;35(2):117-125.
39. Harnud S, Zhang AQ, Yuan ZH. Synthesis of tritium-labeled cyadox , a promising antimicrobial growth-promoting agent with high specific activity. Appl Radiat Isotopes. 2018;139:244-250.
40. Cui LQ, Xing D, Huang DY, Li DY, Lu QR, Wang X, et al. Signaling pathways involved in the expression of SZNF and the target genes binding with SZNF related to cyadox . Biomed Pharmacother. 2018;108:1879-1893.
41. Zhu HL, Yuan ZH, Wang YL, Qiu YS, Fan SX. The effect of cyadox supplementation on metabolic hormones and epidermal growth factor in pigs. Animal Science An International Journal of Fundamental & Applied Research. 2007;82(03):345-350.
42. Kenny FN, Drymoussi Z, Delaine-Smith R, Kao AP, Laly AC, Knight MM, et al. Tissue stiffening promotes keratinocyte proliferation through activation of epidermal growth factor signaling. Journal of Cell Science. 2018;131(10): 215780.
43. Zhou P, Hu J, Wang XQ, Wang JY, Zhang Y, Wang C. Epidermal growth factor receptor expression affects proliferation and apoptosis in non-small cell lung cancer cells via the extracellular signal-regulated kinase/microRNA 200a signaling pathway. Oncology letters. 2018;15(4):5201-5207.
44. Dashtaki ME, Nezhad SRK, Hemadi M, Saki G, Mohammadiasl J. Effects of Epidermal Growth Factor, Glial Cell Line-Derived Neurotrophic and Leukemia Inhibitory Factor on the Proliferation and Differentiation Potential of Adipose Tissue-Derived Mesenchymal Stem Cells. Iranian Red Crescent Medical Journal. 2018;20(1): e55943.
45. Gaviglio AL, Knelson EH, Blobe GC. Heparin-binding epidermal growth factor-like growth factor promotes neuroblastoma differentiation. Faseb J. 2017;31(5):1903-1915.

46. Daughaday WH, Phillips LS, Mueller MC. The effects of insulin and growth hormone on the release of somatomedin by the isolated rat liver. Endocrinology. 1976;98(5):1214.
47. Miura Y, Higashi Y, Kato H, Takahashi S, Noguchi T. Effects of dexamethasone on the production of insulin-like growth factor-I and insulin-like growth factor binding proteins in primary cultures of rat hepatocytes. Journal of the Agricultural Chemical Society of Japan. 1992;56(9):1396-1400.
48. Huat TJ, Khan AA, Pati S, Mustafa Z, Abdullah JM, Jaafar H. IGF-1 enhances cell proliferation and survival during early differentiation of mesenchymal stem cells to neural progenitor-like cells. Bmc Neuroscience. 2014;15: 91.
49. Gao TL, Zhang N, Wang ZL, Wang Y, Liu Y, Ito Y, et al. Biodegradable Microcarriers of Poly(Lactide-co-Glycolide) and Nano-Hydroxyapatite Decorated with IGF-1 via Polydopamine Coating for Enhancing Cell Proliferation and Osteogenic Differentiation. Macromolecular Bioscience. 2015;15(8):1070-1080.
50. Xu N, Huang LL, Liu ZL, Pan YH, Wang X, Tao YF, et al. Metabolism of cyadox by the intestinal mucosa microsomes and gut flora of swine, and identification of metabolites by high-performance liquid chromatography combined with ion trap/time-of-flight mass spectrometry. Rapid Commun Mass Sp. 2011;25(16):2333-2344.
51. Bird A. DNA methylation patterns and epigenetic memory. Genes & Development. 2002;16(1):6-21.
52. Henriksen SD, Madsen PH, Krarup H, Thorlacius-Ussing O. DNA Hypermethylation as a Blood-Based Marker for Pancreatic Cancer A Literature Review. Pancreas. 2015;44(7):1036-1045.
53. Elhamamsy AR. DNA methylation dynamics in plants and mammals: overview of regulation and dysregulation. Cell Biochem Funct. 2016;34(5):289-298.
54. Kader F, Ghai M. DNA methylation and application in forensic sciences. Forensic Sci Int. 2015;249:255-265.
55. Fu Q, Yu X, Callaway CW, Lane RH, McKnight RA. Epigenetics: intrauterine growth retardation (IUGR) modifies the histone code along the rat hepatic IGF-1 gene. Faseb J. 2009;23(8):2438-2449.
56. Herman JG, Baylin SB. Gene silencing in cancer in association with promoter hypermethylation. N Engl J Med. 2003;349(21):2042-2054.
57. Laird PW. The power and the promise of DNA methylation markers. Nat Rev Cancer. 2003;3(4):253-266.
58. Strahl BD, Allis CD. The language of covalent histone modifications. Nature. 2000;403(6765):41-45.
59. Yun MY, Wu J, Workman JL, Li B. Readers of histone modifications. Cell Research. 2011;21(4):564-578.
60. Pinskaya M, Morillon A. Histone H3 lysine 4 di-methylation: a novel mark for transcriptional fidelity? Epigenetics. 2009;4(5):302-306.
61. Heintzman ND, Stuart RK, Hon G, Fu YT, Ching CW, Hawkins RD, et al. Distinct and predictive chromatin signatures of transcriptional promoters and enhancers in the human genome. Nature Genetics. 2007;39(3):311-318.

62. Creyghton MP, Cheng AW, Welstead GG, Kooistra T, Carey BW, Steine EJ, et al. Histone H3K27ac separates active from poised enhancers and predicts developmental state. P Natl Acad Sci USA. 2010;107(50):21931-21936.
63. De Santa F, Barozzi I, Mietton F, Ghisletti S, Polletti S, Tusi BK, et al. A Large Fraction of Extragenic RNA Pol II Transcription Sites Overlap Enhancers. Plos Biology. 2010;8(5): e000384.
64. Cao J, Wu LZ, Zhang SM, Lu M, Cheung WKC, Cai W, et al. An easy and efficient inducible CRISPR/Cas9 platform with improved specificity for multiple gene targeting. Nucleic Acids Research. 2016;44(19): 19.
65. Jakovcevski M, Ruan H, Shen EY, Dincer A, Javidfar B, Ma Q, et al. Neuronal Kmt2a/Mll1 Histone Methyltransferase Is Essential for Prefrontal Synaptic Plasticity and Working Memory. Journal of Neuroscience. 2015;35(13):5097-5108.
66. Hou JL, Wu J, Dombkowski A, Zhang KZ, Holowatyj A, Boerner JL, et al. Genomic amplification and a role in drug-resistance for the KDM5A histone demethylase in breast cancer. American Journal of Translational Research. 2012;4(3):247-256.
67. Huang YC, Shih HY, Lin SJ, Chiu CC, Ma TL, Yeh TH, et al. The Epigenetic Factor Kmt2a/Mll1 Regulates Neural Progenitor Proliferation and Neuronal and Glial Differentiation. Developmental Neurobiology. 2015;75(5):452-462.
68. Zheng F, Kasper LH, Bedford DC, Lerach S, Teubner BJW, Brindle PK. Mutation of the CH1 Domain in the Histone Acetyltransferase CREBBP Results in Autism-Relevant Behaviors in Mice. Plos One. 2016;11(1): e0146366.
69. Rahner N, Brockschmidt FF, Steinke V, Kahl P, Becker T, Vasen HFA, et al. Mutation and association analyses of the candidate genes ESR1, ESR2, MAX, PCNA, and KAT2A in patients with unexplained MSH2-deficient tumors. Familial Cancer. 2012;11(1):19-26.
70. Ravnskjaer K, Hogan MF, Lackey D, Tora L, Dent SYR, Olefsky J, et al. Glucagon regulates gluconeogenesis through KAT2B-and WDR5-mediated epigenetic effects. Journal of Clinical Investigation. 2013;123(10):4318-4328.
71. Wang GL, Salisbury E, Shi X, Timchenko L, Medrano EE, Timchenko NA. HDAC1 cooperates with C/EBPalpha in the inhibition of liver proliferation in old mice. J Biol Chem. 2008;283(38):26169-26178.
72. Risca VI, Denny SK, Straight AF, Greenleaf WJ. Variable chromatin structure revealed by in situ spatially correlated DNA cleavage mapping. Nature. 2017;541(7636):237.
73. Smith OK, Aladjem MI. Chromatin Structure and Replication Origins: Determinants of Chromosome Replication and Nuclear Organization. J Mol Biol. 2014;426(20):3330-3341.

Figures

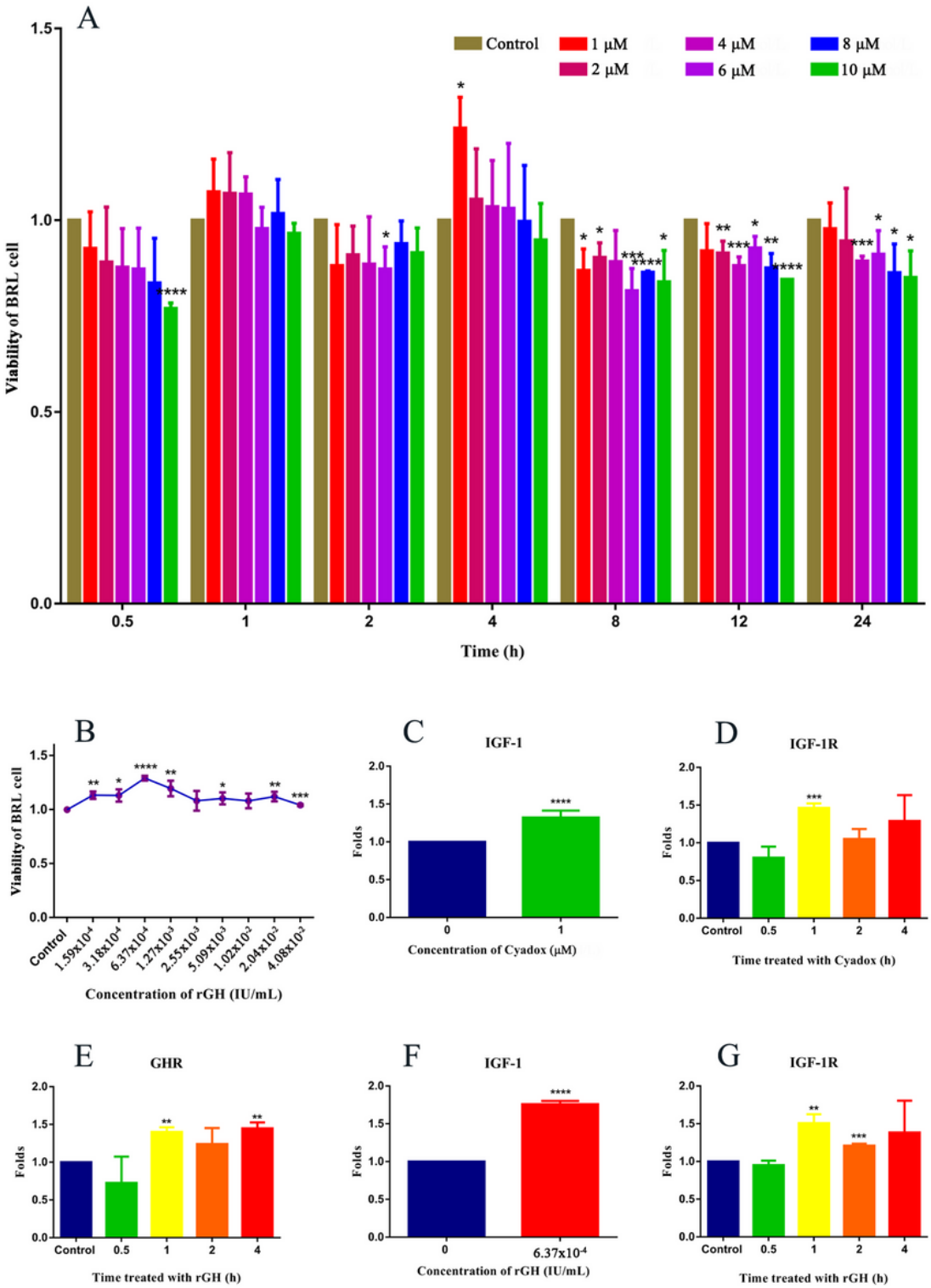

Figure 1

RGH and cyadox treatments affect the growth and development of BRL cells. BRL cells were treated with cyadox (1, 2, 4, 6, 8, and 10 μM) for 0.5, 1, 2, 4, 8, 12, and 24 h and viability of BRL cells was assessed by MTT cell proliferation assay (A). BRL cells were treated with rGH (1.59×10-4, 3.18×10-4, 6.37×10-4, 1.27×10-3, 2.55×10-3, 5.09×10-3, 1.02×10-2, 2.04×10-2 and 4.08×10-2 IU/mL) for 4 h and viability of BRL cells were assessed by MTT cell proliferation assay (B). By RT-PCR, we measured the expression of IGF-1

(C) and IGF-1R (D) following treatment with cyadox (1 μM), and GHR (E), IGF-1 (F), and IGF-1R (G) following treatment with rGH (6.37×10-4 IU/mL). All the results were shown as mean ± SD (n = 3), which were three separate experiments performed in triplicate. Significant differences were indicated by *p < 0.05, **p < 0.01, ***p < 0.0002, ****p < 0.0001, versus control.

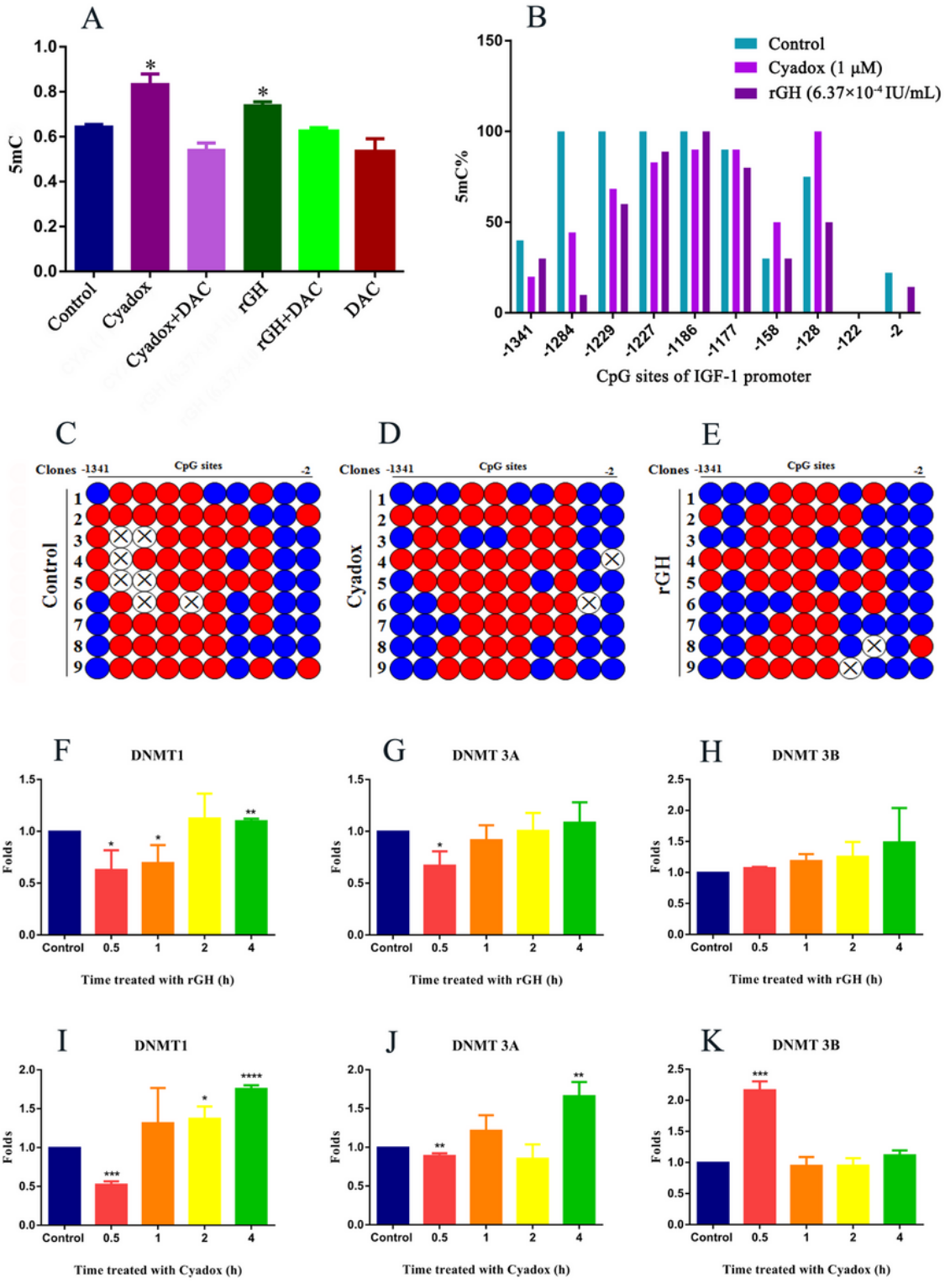

Figure 2

RGH and cyadox treatments affect the methylation level of genomic DNA and the promoter region of IGF-1. The level of DNA methylation (A) in genomic DNA was assessed using MethylFlash Methylated DNA Quantification Kit (Colorimetric) after BRL cells were treated with rGH and cyadox. The level of DNA methylation (B) in promoter regions of IGF-1 was assessed by BSP after BRL cells were treated by rGH and cyadox. Status of DNA methylation in CpG sites of IGF-1 was showed in control group (C), group with treatment of rGH (D), and group with treatment of cyadox (E). DNMT1, DNMT 3A, and DNMT 3B expression levels were assessed by RT-PCR following rGH (6.37×10-4 IU/mL) (F□H) and cyadox (1 μM) (I□K) treatments. All the results were shown as mean ± SD (n = 3), which were three separate experiments performed in triplicate. Significant differences were indicated by *p < 0.05, **p < 0.01, ***p < 0.0002, ****p < 0.0001, versus control..Note: the red dots represent the CpG sites of methylation; the blue dots represent the non methylated CpG sites, and ×represents the mutation sites. -1341, -1284, -1229, -1227, -1186, -1177, -158, -128, -122 and -2 present 1341bp, 1284bp, 1229bp, 1227bp, 1186bp, 1177bp, 158bp, 128bp, 122bp and 2bp at the upstream of promoter 1 of IGF-1.

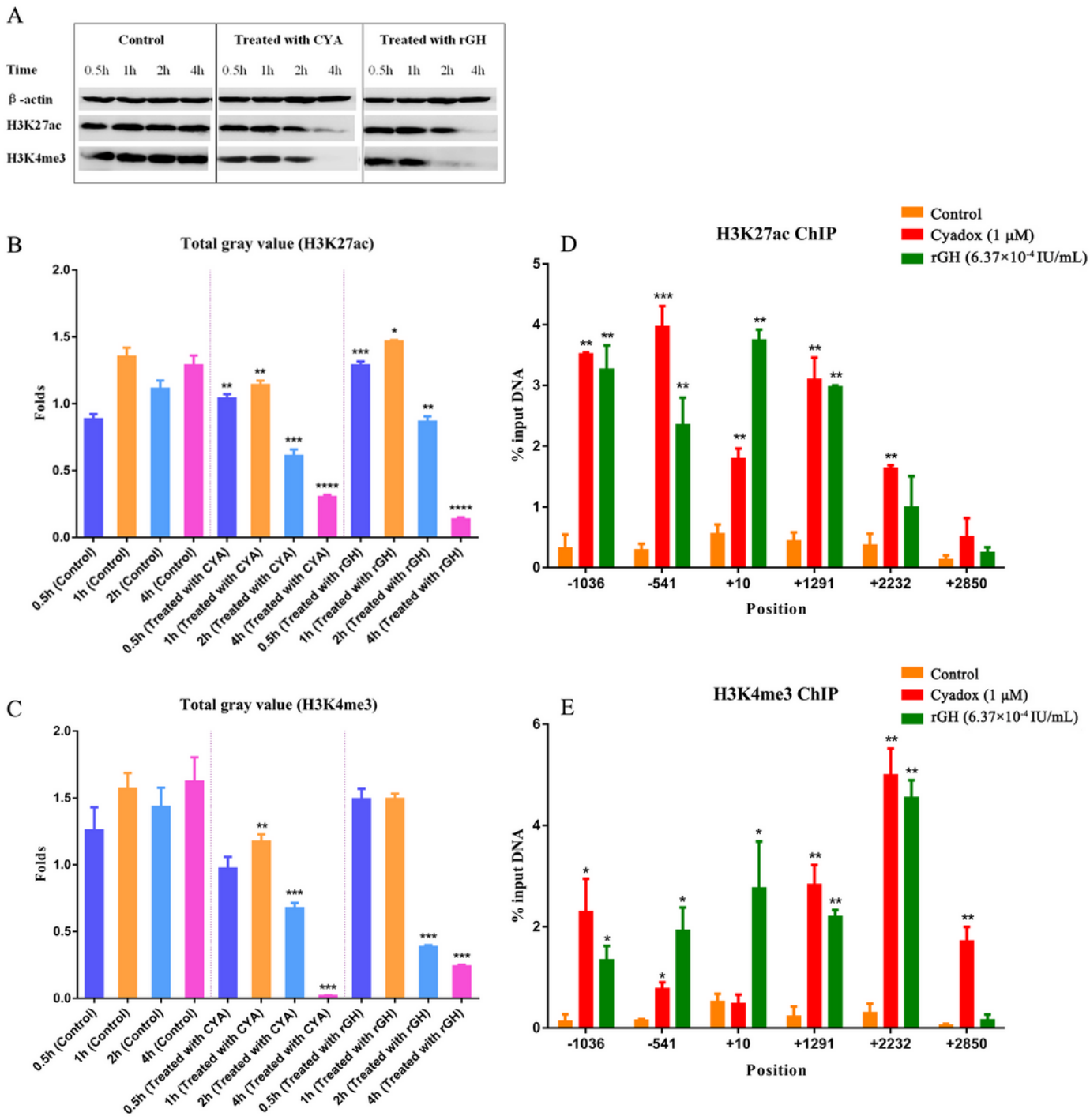

Figure 3

RGH and cyadox treatments affect histone modification level in the promoter region of IGF-1. The level of H3K4me3 and H3K27ac (A) were assessed by western blotting after BRL cells were treated with rGH and cyadox for 0.5, 1, 2 and 4 h. The band intensity values for H3K27ac (B) and H3K4me3 (C) were shown. And level of H3K27ac (D) and H3K4me3 (E) in the promoter regions of IGF-1 were assessed by ChIP-qPCR following rGH and cyadox treatments (4 h). All the results were shown as mean ± SD (n = 3), which were

three separate experiments performed in triplicate. Significant differences were indicated by *p < 0.05, **p < 0.01, ***p < 0.0002, ****p < 0.0001, versus control. Note: -1036, -541 present 1036bp, 541bp at the upstream of promoter 1 of IGF-1. +10, +1291, +2232, +2850 present 10bp, 1291bp, 2232bp, 2850bp at the dowmstream of promoter 1 of IGF-1. -1036, -541 present 1036bp, 541bp at the upstream of promoter 1 of IGF-1. +10, +1291, +2232, +2850 present 10bp, 1291bp, 2232bp, 2850bp at the dowmstream of promoter 1 of IGF-1.

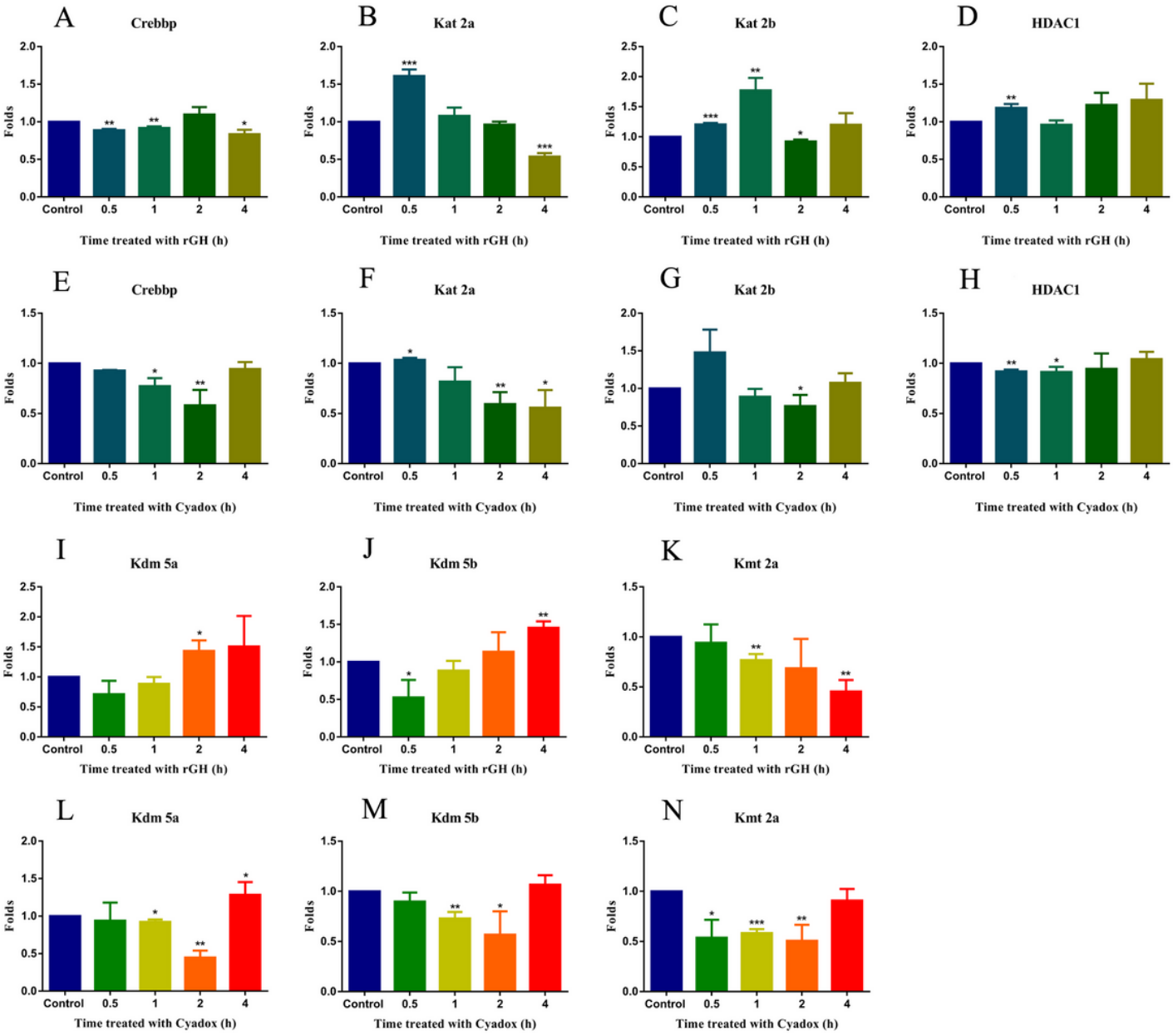

Figure 4

RGH and cyadox treatments lead to the abnormal expression of genes regulated histone modification. The gene expression of Crebbp (A), Kat 2a (B), Kat 2b (C), HDAC1 (D), Kdm 5a (I), Kdm 5b (J) and Kmt 2a (K) with the cells were treated with rGH (6.37×10-4 IU/mL) for 0.5, 1, 2 and 4 h were assessed by RT-PCR. And the gene expression of Crebbp (E), Kat 2a (F), Kat 2b (G), HDAC1 (H), Kdm 5a (L), Kdm 5b (M) and

Kmt 2a (N) were also assessed by RT-PCR with the cells were treated with cyadox (1 μM) for 0.5, 1, 2 and 4 h. All the results were shown as mean ± SD (n = 3), which were three separate experiments performed in triplicate. Significant differences were indicated by *p < 0.05, **p < 0.01, ***p < 0.0002, ****p < 0.0001, versus control.

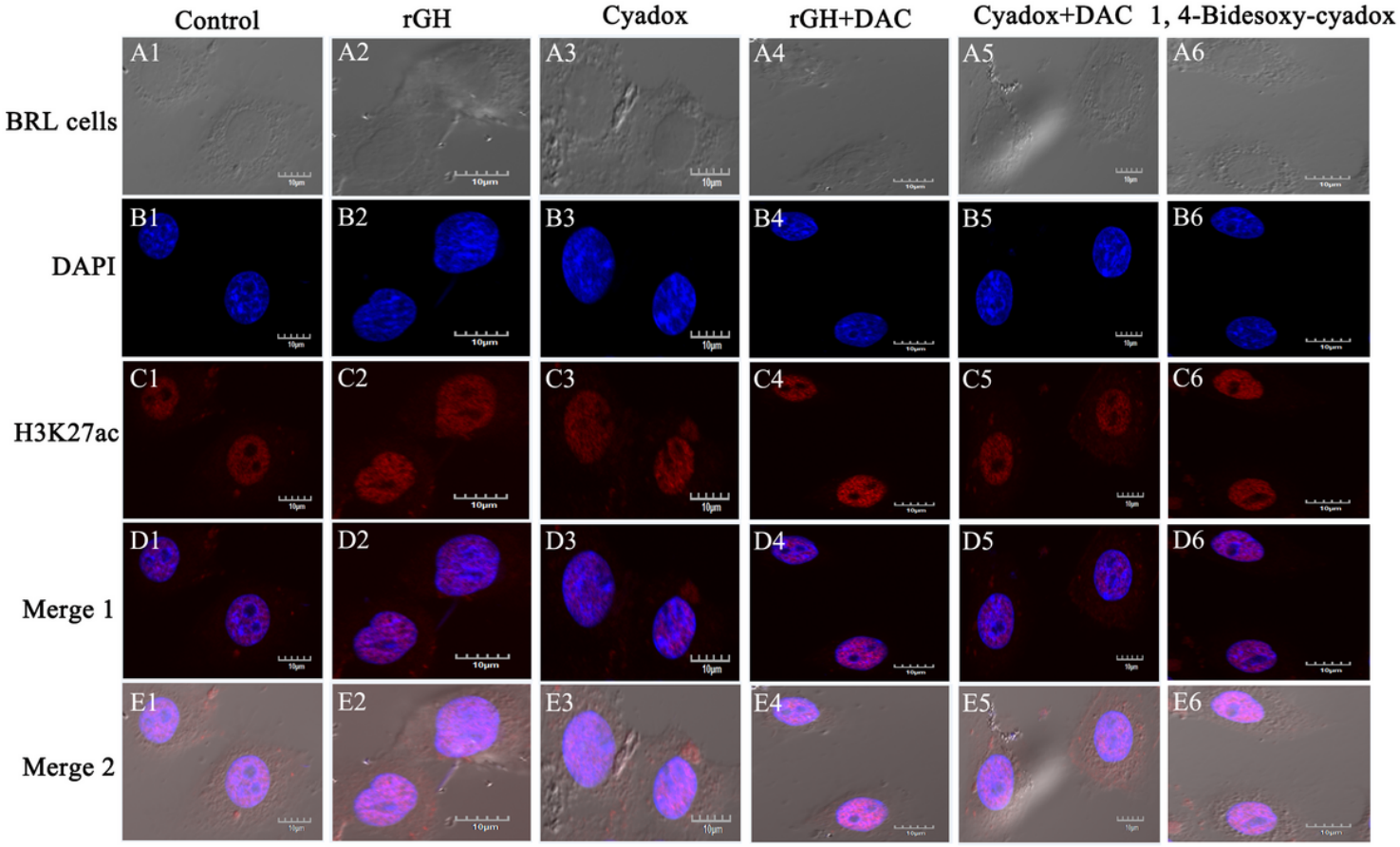

Figure 5

The assay of immunofluorescence about H3K27ac in BRL cells treated with drug-free, rGH (6.37×10-4 IU/mL) cyadox (1 μM), rGH (6.37×10-4 IU/mL) and inhibitor (5-Aza-2'-deoxycytidine, 5 μM), cyadox (1 μM) and inhibitor (5 μM) and 1, 4-Bidesoxycyadox (1 μM), respectively. A1~A6 represent the picture of BRL cells, B1~B6 represent the picture of BRL cells stained with DAPI, C1~C6 represent the picture of BRL cells stained with H3K27ac antibody, D1~D6 represent combination of the picture of BRL cells stained with DAPI and the picture of BRL cells with H3K27ac antibody, E1~E6 represent combination of the picture of BRL cells, the picture of BRL cells stained with DAPI and the picture of BRL cells stained with H3K27ac antibody.

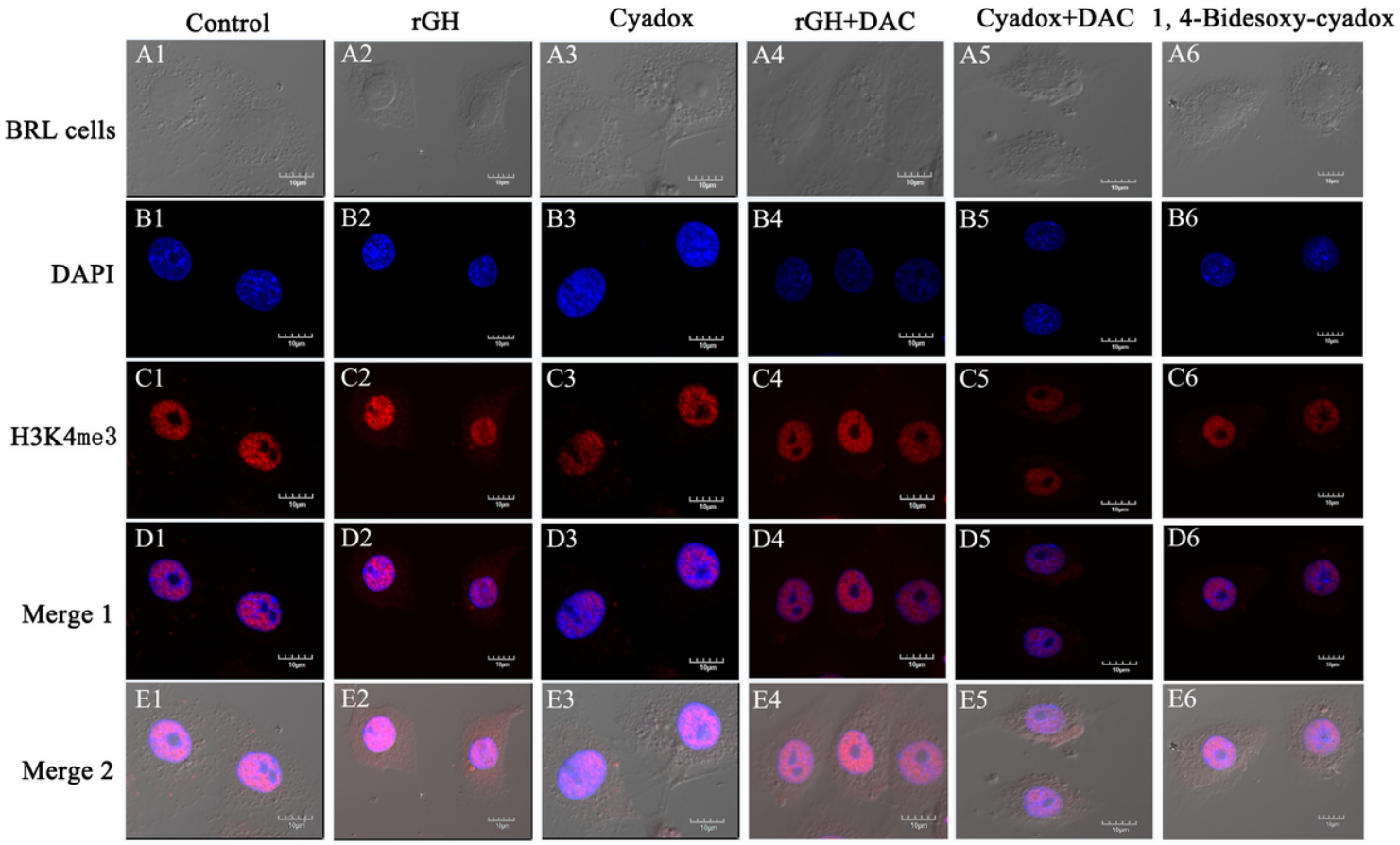

Figure 6

The assay of immunofluorescence about H3K4me3 in BRL cells treated with drug-free, rGH (6.37×10-4 IU/mL), cyadox (1 μM), rGH (6.37×10-4 IU/mL) and inhibitor (5-Aza-2'-deoxycytidine, 5 μM), cyadox (1 μM) and inhibitor (5 μM) and 1, 4-Bidesoxycyadox (1 μM), respectively. A1~A6 represent the picture of BRL cells, B1~B6 represent the picture of BRL cells stained with DAPI, C1~C6 represent the picture of BRL cells stained with H3K4me3 antibody, D1~D6 represent combination of the picture of BRL cells stained with DAPI and the picture of BRL cells with H3K4me3 antibody, E1~E6 represent combination of the picture of BRL cells, the picture of BRL cells stained with DAPI and the picture of BRL cells stained with H3K4me3 antibody.

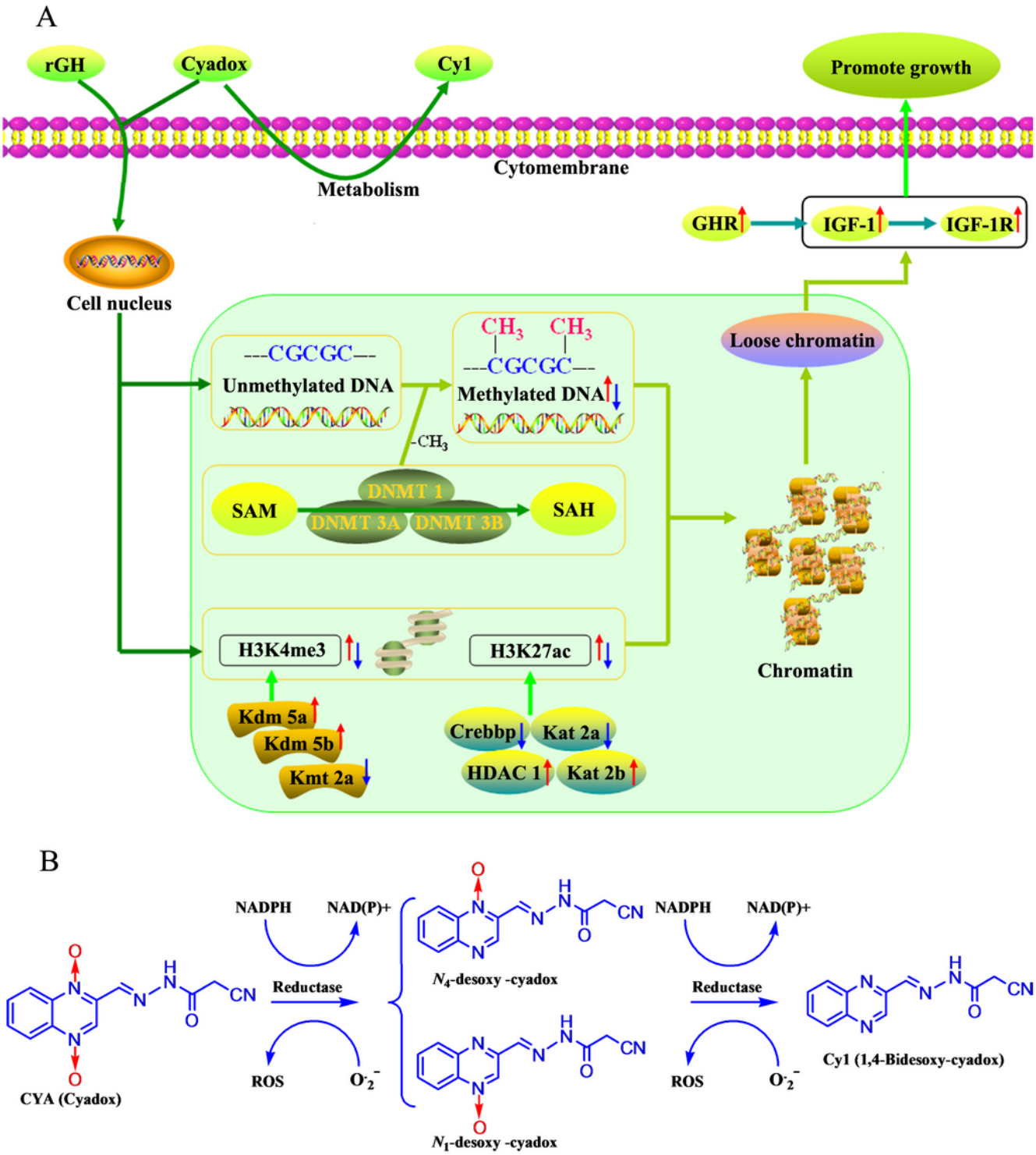

Figure 7

RGH and cyadox promote growth partially through DNA methylation, histone modification and chromatin remodeling. Red upward arrows indicate gene up-regulation. Blue downward arrows indicate gene down-regulation. The relationship between growth and changes of epigenetics induced by cyadox and rGH are showed (A). Cyadox-and rGH-induced hypermethylation of genomic DNA and hypomethylation of the IGF-1 promoter were regulated by DNMT1, DNMT 3A and DNMT 3B. Methyl was from SAM, and SAM became

to SAH after losing a methyl. The decrease in H3K4me3 and increase of H3K4me3 at the IGF-1 promoter following cyadox and rGH treatment were regulated by Kdm 5a, Kdm 5b, and Kmt 2a. Cyadox-and rGH-induced changes in H3K27ac and H3K27ac at the IGF-1 promoter were regulated by Crebbp, Kat 2a, Kat 2b, and HDAC1. The chromatin structure was loosened by cyadox and rGH treatments. CYA can be metabolized into N1-desoxy-cyadox and N4-desoxy-cyadox, and then further metabolized into Cy1 (1, 4-Bidesoxy-cyadox) (B). The metabolism of cyadox might produce ROS, which affects growth and development. Chromatin was unchanged following Cy1 treatment, suggesting a role for cyadox in the observed process of chromatin loosening. In addition, loose chromatin might be reduced by DNA methylation, histone modification, ncRNA, mRNA, procedural expression, transcription factors, pKa in the nucleus and other factors that were influenced by cyadox and rGH. In addition, the formation of IGF-1 gene transcription initiation complex, expression of IGF-1 mRNA and IGF-1R mRNA were promoted with the treatment of cyadox and rGH. The combination of IGF-1 and IGF-1R is a necessary condition to exert the role of IGF-1.